https://ntrs.nasa.gov/search.jsp?R=19800018785 2018-01-30T20:22:31+00:00Z

NASA
TP
1705
c.1

NASA Technical Paper 1705

LOAN COPY: R
AFWL TECHNIC
KIRTLAND AFB

TECH LIBRARY KAFB, NM
0134883

CAS2D - FORTRAN Program for Nonrotating Blade-to-Blade, Steady, Potential Transonic Cascade Flows

Djordje S. Dulikravich

JULY 1980

NASA

TECH LIBRARY KAFB, NM

0134883

NASA Technical Paper 1705

CAS2D - FORTRAN Program for Nonrotating Blade-to-Blade, Steady, Potential Transonic Cascade Flows

Djordje S. Dulikravich
Lewis Research Center
Cleveland, Ohio

National Aeronautics
and Space Administration

Scientific and Technical
Information Office

1980

SUMMARY

An exact, full-potential-equation (FPE) model for the steady, irrotational, homentropic and homoenergetic flow of a compressible, homocompositional, inviscid fluid through two-dimensional planar cascades of airfoils was derived, together with its appropriate boundary conditions.

A computer program, CAS2D, was developed that numerically solves an artificially time-dependent form of the actual FPE. The governing equation was discretized by using type-dependent, rotated finite differencing and the finite area technique. The flow field was discretized by providing a boundary-fitted, nonuniform computational mesh. The mesh was generated by using a sequence of conformal mapping, nonorthogonal coordinate stretching, and local, isoparametric, bilinear mapping functions. The discretized form of the FPE was solved iteratively by using successive line overrelaxation. The possible isentropic shocks were correctly captured by adding explicitly an artificial viscosity in a conservative form. In addition, a four-level, consecutive, mesh refinement feature makes CAS2D a reliable and fast algorithm for the analysis of transonic, two-dimensional cascade flows.

INTRODUCTION

This work is an extension of the author's doctoral research (ref. 1).

The purpose of this report is to give instructions to potential users of the computer program CAS2D. These instructions refer to the possible applications and restrictions of CAS2D. The basic assumptions of the theory used to develop CAS2D are also detailed.

The simplest (although, still exact) mathematical model of the fluid flow is the full potential equation (FPE). Expressed in the two-dimensional Cartesian coordinate system (fig. 1), the FPE can be written as

$$\left(a^2 - \varphi_{,x}^2\right)\varphi_{,xx} + \left(a^2 - \varphi_{,y}^2\right)\varphi_{,yy} - 2\varphi_{,x}\varphi_{,y}\varphi_{,xy} = 0 \tag{1}$$

where a is the local speed of sound and φ is the velocity potential function ($\vec{V} = \vec{\nabla}\varphi$). This equation represents a continuity equation for the steady, irrotational, homentropic flow of an inviscid, homocompositional, compressible fluid. The conditions for

its validity are that no sources of entropy production exist and that the flow is adiabatic. This can be seen from Crocco's formula

$$\vec{V} \times (\vec{\nabla} \times \vec{V}) = \vec{\nabla}H - T\,\vec{\nabla}S \tag{2}$$

where $\vec{V} = u\hat{e}_x + v\hat{e}_y$ is the velocity vector; H, the total enthalpy; T, the absolute temperature; S, the entropy; and

$$\vec{\nabla} \times \vec{V} = 0 \tag{3}$$

the irrotationality condition.

In practice, this means that the flow is uniform (irrotational) at upstream infinity and that all the viscous effects are confined to a narrow, nonseparated boundary-layer region. The flow at downstream infinity should also be uniform in accordance with the steady-flow inviscid theory.

In actual viscous flows the vorticity created at the solid boundary is convected and diffused downstream, where it forms a wake. The velocity deficit in the wake rapidly disappears. Therefore it is reasonable to assume that the downstream infinity is only a few chord lengths from the trailing edge.

The discontinuities possible in the solution of FPE are isentropic shocks. They do not represent physical shock waves (ref. 2) because they do not satisfy Rankine-Hugoniot jump conditions. Nevertheless they are of approximately correct strength and at approximately the correct position if the Mach number just ahead of the discontinuity is less than about 1.3.

The results obtained by this two-dimensional analysis are not directly applicable to three-dimensional, potential, rotating flows through a cascade of blades. The reason is that the Coriolis force does not exist in two-dimensional, potential, cascade flows.

ANALYSIS

Transonic, Full Potential Equation

The continuity equation for steady flow with no sources or sinks in the flow field is

$$\vec{\nabla} \cdot (\rho\vec{V}) = \vec{V} \cdot (\vec{\nabla}\rho) + \rho(\vec{\nabla} \cdot \vec{V}) = 0 \tag{4}$$

where ρ is the local fluid density and $\vec{V}$ is the local fluid velocity vector

$$\vec{V} = u\hat{e}_x + v\hat{e}_y \tag{5}$$

For continuous, homentropic flow of a homocompositional fluid the relation

$$\frac{\vec{\nabla}h}{a^2} = \frac{\vec{\nabla}\rho}{\rho} \tag{6}$$

is valid, where h is the local static enthalpy and a is the local speed of sound

$$a^2 = \left(\frac{\partial p}{\partial \rho}\right)_{\text{isentropic}} \tag{7}$$

After premultiplying equation (4) by a^2/ρ and taking into account equation (6), we get

$$a^2(\vec{\nabla} \cdot \vec{V}) + \vec{V} \cdot (\vec{\nabla}h) = 0 \tag{8}$$

In general

$$h = H - \frac{V^2}{2} \tag{9}$$

where the total enthalpy H must be constant throughout the flow field in order to preserve the irrotationality condition (eq. (2)).

Then equation (8) becomes

$$a^2(\vec{\nabla} \cdot \vec{V}) - (\vec{V} \cdot \vec{\nabla})Q = 0 \tag{10}$$

where

$$Q = \frac{|\vec{V}|^2}{2} \tag{11}$$

The continuity equation (10) can be written in its quasi-conservative scalar form (ref. 3) as

$$a^2(u_{,x} + v_{,y}) - (uQ_{,x} + vQ_{,y}) = 0 \tag{12}$$

or in its fully conservative scalar form as

$$\frac{\rho}{a^2}\left((\rho u)_{,x} + (\rho v)_{,y}\right) = 0 \tag{13}$$

With introduction of the velocity potential, equation (10) becomes the full-potential equation

$$\left(a^2 - \varphi_{,x}^2\right)\varphi_{,xx} + \left(a^2 - \varphi_{,y}^2\right)\varphi_{,yy} - 2\varphi_{,x}\varphi_{,y}\varphi_{,xy} = 0 \tag{14}$$

Equation (14) is a quasi-linear, second-order partial differential equation of the mixed (elliptic-hyperbolic) type. Its canonical form (ref. 4) is

$$(a^2 - q^2)\varphi_{,ss}^H + a^2\left(\nabla^2\varphi^E - \varphi_{,ss}^E\right) = 0 \tag{15}$$

where the superscript H designates upstream differencing and the superscript E designates the central differencing that should be used in the discretization of equation (15). Here, s is the streamline direction and

$$q^2 = (u^2 + v^2) \tag{16}$$

For the finite difference evaluation of the derivatives, the flow field and the governing equations were transformed into a rectangular (X, Y) computational space (fig. 4). The transformation matrix is

$$[J]^T = \begin{bmatrix} x_{,X} & y_{,X} \\ x_{,Y} & y_{,Y} \end{bmatrix} \tag{17}$$

Then the modified contravariant velocity components are

$$\begin{Bmatrix} U \\ V \end{Bmatrix} = D[J]^{-1}\begin{Bmatrix} u \\ v \end{Bmatrix} = D[B]\begin{Bmatrix} \varphi_{,X} \\ \varphi_{,Y} \end{Bmatrix} \tag{18}$$

where $D = \det[J]$ and

$$[B] = [J]^{-1}\left[J^T\right]^{-1} \tag{19}$$

Consequently the fully conservative form of the continuity equation (eq. (13)) becomes

$$\frac{\rho}{a^2}\left((\rho U)_{,X} + (\rho V)_{,Y}\right) = 0 \tag{20}$$

where

$$\rho = \left(1 + \frac{\gamma - 1}{2} M_{-\infty}^2 (1 - q^2)\right)^{1/(\gamma-1)}$$

and

$$a^2 = \left(\frac{1}{M_{-\infty}^2}\right) + \frac{\gamma - 1}{2}(1 - q^2)$$

The quasi-conservative form (ref. 3) becomes

$$a^2(U_{,X} + V_{,Y}) - (UQ_{,X} + VQ_{,Y}) = 0 \tag{21}$$

The principal part of the full-potential form (ref. 4) of the continuity equation (eq. (14) or (15)) transforms into

$$S_{XX}\varphi^E_{,XX} + S_{YY}\varphi^E_{,YY} + S_{XY}\varphi^E_{,XY} + R_{XX}\left(\varphi^H_{,XX} - \varphi^E_{,XX}\right) + R_{YY}\left(\varphi^H_{,YY} - \varphi^E_{,YY}\right)$$
$$+ R_{XY}\left(\varphi^H_{,XY} - \varphi^E_{,XY}\right) = 0 \tag{22}$$

where the superscript H designates upstream (or backward) differencing and the superscript E designates central differencing. The coefficients of this equation are as follows:

$$
\left.
\begin{aligned}
\mu &= \max\left(1 - \frac{a^2}{q^2};\ 0.\right) \\
S_{XX} &= a^2 DB_{11} - \frac{U^2}{D} \\
S_{YY} &= a^2 DB_{22} - \frac{V^2}{D} \\
S_{XY} &= 2\left(a^2 DB_{12} - \frac{UV}{D}\right) \\
R_{XX} &= -\frac{\mu U^2}{D} \\
R_{YY} &= -\frac{\mu V^2}{D} \\
R_{XY} &= -\frac{2\mu UV}{D}
\end{aligned}
\right\} \tag{23}
$$

For a locally subsonic flow all the second derivatives will be evaluated by central differencing. Upstream differencing (as indicated in eqs. (15) and (22)) is a numerical attempt to simulate the exact shape of the upstream-facing domain of dependence of the locally hyperbolic full-potential equation. It can be shown (ref. 5) that this procedure introduces a numerical truncation error called artificial viscosity, which is proportional to $\varphi_{,SSS}$.

This artificial viscosity term was added to equation (20) or (21) in a conservative form

$$
RVISC = f^H_{,X} + g^H_{,Y} \tag{24}
$$

where

$$f_{i,j} = -\frac{\Delta X}{2}\left(2R_{XX}\varphi^{E}_{,XX} + R_{XY}\varphi^{E}_{,XY}\right) \tag{25}$$

$$g_{i,j} = -\frac{\Delta Y}{2}\left(R_{XY}\varphi^{E}_{,XY} + 2R_{YY}\varphi^{E}_{,YY}\right) \tag{26}$$

The conservative form of RVISC assures the unique position and strength (ref. 2) of the possible isentropic discontinuities in the solution of the governing equation.

Boundary Conditions

The boundary conditions for equation (14) (or (15)) that are valid in the present analysis of a two-dimensional cascade flow are the following: On the airfoil surface the condition is

$$\vec{\nabla}\varphi \cdot \vec{\nabla}F = 0 \tag{27}$$

where $F = F(x, y)$ is the equation of the airfoil contour line. At axial infinities ($x = \pm\infty$) the flow is assumed to be uniform. The upstream boundary condition is incorporated in the special form of the potential function (ref. 4).

$$\varphi(x, y) = (x \cos \alpha_{-\infty} + y \sin \alpha_{-\infty}) + G(x, y) \tag{28}$$

where $\alpha_{-\infty}$ and $\alpha_{+\infty}$ are the angles between the free stream and the x axis at the upstream and downstream infinities, respectively. The term $G(x, y)$ is a so-called "reduced potential" describing the disturbances with respect to the free stream at upstream infinity. All the velocities have been normalized with respect to the magnitude of the free-stream velocity vector at upstream infinity. Hence the boundary condition at upstream infinity ($x = -\infty$) is

$$\left(\varphi, x\right)_{-\infty} = \cos \alpha_{-\infty} \tag{29}$$

$$\left(\varphi, y\right)_{-\infty} = \sin \alpha_{-\infty} \tag{30}$$

That is,

$$(G)_{-\infty} = \text{Constant} \tag{31}$$

where the arbitrary constant is taken as zero.

Conditions that should be applied along the identically shaped and periodically spatially positioned boundaries (corresponding to the lines $\overline{cd}$ and $\overline{ab}$ in fig. 1) represent the physical fact that the velocity vector is a periodic function in a cascade flow

$$\vec{V}(x, y) = \vec{V}(x, y + h) \tag{32}$$

According to the definition of the velocity potential

$$\varphi_d = \varphi_a + \int_a^d \vec{\nabla}\varphi \cdot d\vec{\ell} \tag{33}$$

where

$$d\vec{\ell} = dx\, \hat{e}_x + dy\, \hat{e}_y \tag{34}$$

and because

$$\int_a^b = -\int_c^d \tag{35}$$

it follows that

$$\varphi_d = \varphi_a + \int_b^c (\vec{\nabla}\varphi \cdot d\vec{\ell})_{-\infty} \tag{36}$$

or

$$(\varphi_d - \varphi_a) = h \sin \alpha_{-\infty} \tag{37}$$

From equation (18) it follows that

$$(\varphi_d - \varphi_a) = (x_d - x_a)\cos \alpha_{-\infty} + (y_d - y_a)\sin \alpha_{-\infty} + (G_d - G_a) \tag{38}$$

Because $(x_d - x_a) = 0$ and $(y_d - y_a) = h$, it follows from equations (27) and (28) that the boundary conditions along the periodic boundaries are

$$G(x, y) = G(x, y + h) \tag{39}$$

The global mass conservation is expressed as (fig. 2)

$$h_{-\infty}\rho_{-\infty}q_{-\infty} \cos \alpha_{-\infty} = h_{+\infty}\rho_{+\infty}q_{+\infty} \cos \alpha_{+\infty} \tag{40}$$

where ρ is density and q is the magnitude of the velocity vector. Because $\rho_{-\infty} = 1$ and $q_{-\infty} = 1$,

$$f(q_{+\infty}) = \rho_{+\infty}q_{+\infty} \cos \alpha_{+\infty} - \cos \alpha_{-\infty} = 0 \tag{41}$$

if $h_{-\infty} = h_{+\infty}$. Hence

$$f'(q_{+\infty}) = \rho_{+\infty} \cos \alpha_{+\infty} + q_{+\infty} \cos \alpha_{+\infty}\left(\frac{\partial \rho_{+\infty}}{\partial q_{+\infty}}\right) \tag{42}$$

By using a simple Newton-Raphson iterative technique

$$q_{+\infty}^{n+1} = q_{+\infty}^{n} - \frac{f\left(q_{+\infty}^{n}\right)}{f'\left(q_{+\infty}^{n}\right)} \tag{43}$$

the value of $q_{+\infty}$ can be easily determined. Then the boundary condition at the downstream infinity becomes

$$\left(G_{,x}\right)_{+\infty} = q_{+\infty} \cos \alpha_{+\infty} - \cos \alpha_{-\infty} \tag{44}$$

For lifting flows the potential function becomes multivalued. This problem can be resolved by inserting an arbitrarily shaped cut of zero thickness in the flow field in such a way that it connects the airfoil with the infinity (fig. 1). This cut is conveniently assumed to leave the trailing edge. The finite discontinuity in the velocity potential $\Delta\varphi$ at the trailing edge is equal to the circulation Γ of the velocity field. This constant discontinuity should be preserved (i. e., there should be no jump in the

static pressure) at every point of the cut all the way to the downstream infinity. The exact value of Γ can be calculated from the input data and the value of $q_{+\infty}$ (eq. (33)).

$$\Gamma = \Delta\varphi = h(\sin \alpha_{-\infty} - q_{+\infty} \sin \alpha_{+\infty}) \tag{45}$$

NUMERICAL METHOD

Computational Mesh Generation

The computational mesh (fig. 3) was generated by using a conformal mapping function of the form

$$\tilde{w} = e^{i\beta} \ln\left(\frac{m - \tilde{z}}{m + \tilde{z}}\right) + e^{-i\beta} \ln\left(\frac{1 - m\tilde{z}}{1 + m\tilde{z}}\right) \tag{46}$$

It conformally maps a unit circle with a slit in the middle (ref. 6) whose endpoints are situated at $\tilde{z} = \pm m$ onto the cascade of slits in the $\tilde{w} = x + iy$ plane.

The slits are spaced $2\pi \cos \beta$ apart, where β is the stagger angle of the cascade of slits (fig. 4). The unit circle with a slit in the $\tilde{z} = \xi + i\eta$ plane can be "unwrapped" by using elliptic polar coordinates (ref. 7):

$$\xi = m \cosh u_e \cos v_e \tag{47}$$

$$\eta = m \sinh u_e \sin v_e \tag{48}$$

The resulting (u_e, v_e) plane can be transformed to the rectangular, computational (X, Y) domain with the help of a nonorthogonal shearing transformation (fig. 4) of the general form

$$Y = \frac{u_e}{T(v_e)} \tag{49}$$

$$X = v_e + Y * DRD \tag{50}$$

In the case of an airfoil of nonzero thickness and arbitrary camber, the domain outside the airfoil in $\tilde{w} = x + iy$ space will map onto a nearly circular domain in the

$\tilde{z} = \xi + i\eta$ plane. The consequent introduction of elliptic coordinates will not help to eliminate the problem of mesh nonorthogonality, and one side of the computational rectangle will be an irregular line.

The shape of the mesh cells at axial infinities (fig. 3) was determined explicitly (ref. 1) in order to make the application of the proper boundary conditions (eqs. (31), (39), and (44)) easier.

Finite Area Method

A uniform orthogonal mesh in the (X, Y) computational space remaps into a nonorthogonal mesh in the (x, y) physical space (fig. 3). The local, bilinear, isoparametric mapping functions of the general form

$$b = \frac{1}{4} \sum_{p} b_p (1 + \overline{X}\overline{X}_p)(1 + \overline{Y}\overline{Y}_p) \tag{51}$$

where

$$\left.\begin{aligned} \overline{X}_p &= \pm 1 \\ \overline{Y}_p &= \pm 1 \end{aligned}\right\} \text{where } p = 1, 2, 4, 5 \tag{52}$$

and b stands for x, y or G(x, y), will map each unit square mesh cell from the (X, Y) computational rectangle (fig. 5) into a corresponding distorted mesh cell in the (x, y) physical plane.

The mass flux balance must be satisfied within each auxiliary control cell (ACC), which is represented as a shaded region in figure 5 and centered around each mesh point. This cell is formed from parts of the four neighboring elementary mesh cells (EMC). Each EMC was separately mapped from the (x, y) space to the (X, Y) space. Therefore the value of the desired parameter at the center of each mesh face of that ACC (points N, S, E, W) is evaluated as an arithmetic mean (ref. 3) of the four separate results that are calculated on the basis of the local mapping functions in each of the four neighboring EMC's.

Artificial Time Concept

An attempt to solve the steady, full-potential equation - as an asymptotic solution of the exact, physically unsteady, full-potential equation for long times - would be

very uneconomical because of the small time steps required by the numerical stability considerations. Instead it is customary to use an artificial time-dependent equation (ref. 4) of the form

$$\left(M_r^2 - 1\right)\varphi_{,ss} - \varphi_{,nn} + 2\alpha_1\varphi_{,st} + 2\alpha_2\varphi_{,nt} + \varepsilon\varphi_{,t} = 0 \tag{53}$$

This time-dependent process does not model the true time evolution of the flow. The major advantage of this technique, however, is that the consistency and accuracy of the numerical method used in determining the transient solutions are irrelevant - the consistency being finally achieved asymptotically when the solution no longer depends on time.

Artificially time-dependent differencing was used in a way suggested by Jameson (ref. 5), who considered iteration sweeps through the computational field as successive intervals in an artificial time. Using the successive line overrelaxation (SLOR) technique requires introduction of a temporary or provisional value of the potential φ at every mesh point on the line along which SLOR is to be applied. The definition of such a term is

$$\varphi_{i,j} = \frac{1}{\omega}\varphi^{+}_{i,j} + \left(1 - \frac{1}{\omega}\right)\varphi^{o}_{i,j} \tag{54}$$

where ω is the overrelaxation factor (ref. 4), $\varphi^{+}_{i,j}$ is the new value of the potential (i.e., one that will be obtained as the result of the current iteration sweep), and $\varphi^{o}_{i,j}$ is the old value of the potential (obtained after the previous iteration sweep). According to the numerical stability analysis (ref. 5), factor ω has values less then 2 when the flow is locally subsonic and equal to 2 when the flow is locally supersonic.

The generation of the artificial time derivatives is illustrated in the following example. It is easy (refs. 4 and 1) to check that

$$\left(\varphi_{,XX}\right)^{E}_{i,j} = \left(\varphi^{o}_{i+1,j} - 2\varphi_{i,j} + \varphi^{+}_{i-1,j}\right)\frac{1}{(\Delta X)^2} \tag{55}$$

represents

$$\left(\varphi_{,XX}\right)^{E}_{i,j} = \left(\varphi^{o}_{,XX}\right)^{E}_{i,j} - \frac{\Delta t}{\Delta X}\left(\varphi_{,Xt}\right)_{i-\frac{1}{2},j} - \left(\frac{2}{\omega} - 1\right)\frac{\Delta t}{(\Delta X)^2}\left(\varphi_{,t}\right)_{i,j} \tag{56}$$

and that the expression

$$\left(\varphi, XX\right)^{H}_{i,j} = \left(2\varphi^{+}_{i,j} - \varphi^{o}_{i,j} - 2\varphi^{+}_{i-1,j} + \varphi^{o}_{i-2,j}\right) \frac{1}{(\Delta X)^2} \tag{57}$$

represents

$$\left(\varphi, XX\right)^{H}_{i,j} = \left(\varphi^{o}, XX\right)^{H}_{i,j} + 2\frac{\Delta t}{\Delta X}\left(\varphi, Xt\right)_{i-\frac{1}{2},j} \tag{58}$$

where the superscripts E and H represent the central and upstream differencing, respectively.

The vector of the corrections $\left\{C_j\right\}$ to the potential φ was determined from

$$[\delta]\left\{C_j\right\} = \left\{R_j\right\} \tag{59}$$

where the tridiagonal $[\delta]$ matrix of coefficients was determined from equations (22), (23), and (54). The vector of residues $\left\{R_j\right\}$ was determined from equations (21) and (24).

COMPUTER PROGRAM

General Description

The computer program CAS2D consists of 10 routines and a separate input data operation (fig. 6). The input data are discussed in detail in the following section.

The subroutine MAIN is the principal part of CAS2D in the sense that all other routines are called from that routine. MAIN reads the input data and rotates the airfoil to its actual stagger angle. This routine also calculates the length of the central slit in the circle-plane (fig. 4) and interpolates the symmetrically spaced points on the unwrapped surface of the airfoil in the (u_e, v_e) plane (fig. 4). Furthermore MAIN calculates (iteratively) the flow parameters at downstream infinity. It also determines the exact value of the circulation Γ (eq. (45)). Routine MAIN also tests the convergence rate of the iterative process by comparing the value of the expression $(\Gamma^{n+1} - \Gamma^{n})/\Gamma^{n}$ with the prespecified convergence-rate input parameter called CONVER.

Subroutine CONMAP iteratively performs the point-by-point conformal mapping (eq. (46)) from the (x, y) plane onto the circle-plane (ξ, η) (fig. 4). Furthermore CONMAP "unwraps" the circle and calculates the elliptic polar coordinates u_e and v_e (fig. 4).

Subroutine SPLIF fits a cubic spline through the lower boundary of the computational domain in the (u_e, v_e) plane, which corresponds to the surface of the airfoil.

Subroutine INTPL interpolates the values of the elliptic polar coordinates in the (u_e, v_e) plane at points that are equidistantly spaced in the X-direction in the (X, Y) computational plane with respect to the image of the upstream infinity (X = 0; Y = 0). This is a necessary step in obtaining a grid that is periodic in the vertical direction in the (x, y) plane.

Subroutine REMAP analytically determines coordinates of the mesh points in the physical plane; that is, REMAP performs a backtransformation process from the (X, Y) plane to the (x, y) plane.

The mesh points defining the axial infinities should be positioned along the line x = Constant (fig. 3 and eq. (31)). Because of the way that the potential jump Γ is enforced across the cut, the points at $x = +\infty$ should be equidistantly positioned in the y direction with respect to that cut (fig. 3).

Subroutine XYINF determines the coordinates of the axial infinity points explicitly because they cannot be obtained from the conformal mapping. XYINF also determines the coordinates of points in the imaginary rows and columns outside the actual computational domain.

Subroutine XSWEEP iteratively performs the actual flow calculation by using the SLOR technique. XSWEEP uses type-dependent rotated finite differencing (eq. (22)) and the artificial time concept in order to evaluate coefficients of the tridiagonal correction to the potential matrix. The residues are evaluated by using the finite area technique (eqs. (20) or (21)). The artificial viscosity is added explicitly in conservative form (eq. (24)). The form of finite differencing (i. e., the fully conservative scheme (eq. (20)) versus the quasi-conservative scheme (eq. (21)) is indicated at the beginning of each of the two versions of the XSWEEP routine. The choice of the version of the XSWEEP routine that should be used depends on the user. Both versions give practically identical results for the moderately shocked flows. At the same time the fully conservative version takes about 50 percent more execution time.

Subroutine BOUND applies boundary and periodicity conditions after each complete sweep through the flow field performed by XSWEEP. BOUND is also called after each mesh refinement.

Subroutine CPMACH calculates a Mach number at every mesh point in the flow field and prints a Mach number chart after the iterative calculation process has con-

verged on the final grid. CPMACH also calculates and prints out values of the iteratively obtained Mach number, density, and flow angle at the downstream infinity, which can be compared with the exact values obtained from MAIN.

If the iterative calculation process is to be repeated on the next finer mesh, subroutine MESH is called. MESH doubles the number of mesh cells in each direction (X and Y) and interpolates the values of the reduced potential G(x, y) (obtained on the previous grid) onto the new grid, thus creating an improved initial guess for the iterative process on that refined grid.

Input

The first card of the input data contains an arbitrary text with up to 80 characters describing the airfoil or the test case. The actual input parameters, which specify the flow and geometry, are given as real numbers.

The second card contains XCELL, YCELL, and PMESH, where

XCELL — number of mesh cells on surface of airfoil for coarse grid. The number of mesh cells must be an even number; the suggested minimum value is

$$\text{XCELL} = 16.$$

YCELL — number of elliptic layers of mesh cells enveloping airfoil, that is, half the number of mesh cells between two neighboring blades (for coarse grid). The suggested minimum value is

$$\text{YCELL} = 4.$$

PMESH — total number of grids used. The present version of CAS2D is capable of calculating on a coarse grid and three consecutively refined grids. Hence the maximum allowable value is

$$\text{PMESH} = 4.$$

The third card contains ALPHA1, TWIST, and ALPHA2, where

ALPHA1, ALPHA2 — angle, $\alpha_{-\infty}$, $\alpha_{+\infty}$ (in degrees) between x-axis and free stream at up- and downstream infinity, respectively (fig. 1)

TWIST — stagger angle, β (in degrees) between x-axis and airfoil chord line (fig. 1)

The fourth card contains PITCH, RO1, and RO2, where

PITCH gap-chord ratio, h/c (fig. 1). The iterative determination of certain parameters in the mesh-generating routines might fail for small values of PITCH because of the computer-dependent accuracy. Therefore it is suggested that CAS2D be used for cascades with

$$\text{PITCH} > 0.65$$

RO1, RO2 radii (dimensionless) of airfoil at leading and trailing edges, respectively. For theoretically zero radii with respect to chord length, use

$$\text{RO1} = 1.*10^{-4}$$

$$\text{RO2} = 1.*10^{-4}$$

The fifth card contains FMACH, CONVER, and AR, where

FMACH Mach number $M_{-\infty}$ of free stream at upstream infinity. The maximum allowed value is

$$\text{FMACH} = 0.99$$

This value should be lowered if it produces a shock that has a Mach number just ahead of it greater than ~1.3.

RLX overrelaxation factor (eq. (54)) on coarse grid for case of locally subsonic flow. The suggested value is

$$\text{RLX} = 1.75$$

This value will be automatically increased by 4 percent on each consecutively finer grid. In the locally supersonic flow, the relaxation factor is automatically taken as

$$\text{RLX} = 2.$$

AR ratio of inlet area to exit area of blade-to-blade passage (fig. 2),

$$\text{AR} = (hh_{-\infty}/hh_{+\infty})$$

The input parameter AR should provide the appropriate value of the downstream Mach number. For an airfoil with a closed trailing edge, use

$$AR = 1.$$

If the airfoil has an open trailing edge extending to downstream infinity (e. g., shockless airfoils obtained from the design method of ref. 8), the approximate value of AR could be calculated from the known thickness δ_W of the trailing edge,

$$AR = 1. + (\delta_W/PITCH)$$

The sixth input card contains TITR1, TITR2, and TITR3, where

TITR1, TITR2, TITR3 — maximum number of iterations on each of the first three grids, respectively. These three parameters are important because they serve as a convergence criterion in the case of nonlifting flows ($\Gamma < 1. *10^{-6}$). The suggested values that will provide results with engineering accuracy are

$$TITR1 = 150.$$

$$TITR2 = 60.$$

$$TITR3 = 30.$$

In the case that PMESH = 4, the maximum number of iterations on the fourth grid will be automatically taken as TITR3/2.

The seventh input card contains POINTS, GAMMA, and CONVER, where

POINTS — number of input mesh points on surface of airfoil. For a nonsymmetric airfoil, POINTS must be an odd number (counting the trailing-edge point twice). For a symmetric airfoil only an even number of points defining its lower surface should be given as input (counting the trailing-edge and leading-edge points once only). The maximum total number of input points in the present version of CAS2D is

$$POINTS = 129.$$

Note that the number of the input points on the airfoil lower surface does not have to be the same as the number of the input points on its upper surface. Before preparing the input data it might be helpful to consult the four examples shown in the appendix.

GAMMA ratio of specific heats of working fluid

CONVER circulation rate of convergence criteria in case of lifting flows

$$\text{CONVER} = \left| \frac{(\Gamma^{n+1} - \Gamma^{n})}{\Gamma^{n}} \right|$$

The suggested input value is

$$\text{CONVER} = 1. * 10^{-5}$$

The x' and y' coordinates of input points on the surface of an airfoil in the cascade are given on the rest of the input cards starting with the eighth card. These coordinates will be normalized with respect to the airfoil chord length. The input coordinate system (x', y') could be arbitrarily positioned with respect to the airfoil (fig. 7).

The input points are numbered in the clockwise direction starting from the trailing-edge point. The numbering must end with the same trailing-edge point for a nonsymmetric airfoil and with the leading-edge point for a symmetric airfoil. The coordinates are printed on input cards in such a way that x' coordinates of all the input points are given in the first column, followed by the corresponding y' coordinates in the second column (see appendix).

Output

The results of the CAS2D computer program appear in printed form only. There are no output files stored in the computer.

First, the printout gives the name of the program, the name of the programmer, and the name of the airfoil or test case as specified on the first input data card.

The four columns that appear next show normalized x' and y' coordinates prerotated to a zero stagger angle (in the first two columns) and as they appear after rotating the airfoil for the value of stagger angle TWIST (in the last two columns).

Next, the values of the flow parameters at the downstream infinity are given. They are obtained from an iterative procedure involving the input flow parameters and the mass conservation principle.

It is possible to monitor the iterative process by using the following parameters, which are printed after each complete iterative sweep through the flow field. These parameters are

ITER	number of iteration sweep just completed
IR, JR	coordinates of point where residue had largest absolute value
MAX· RESIDUE	maximum residue (eq. (20) or (21) plus (24) in flow field. Its location is at the point (IR, JR).
IC, JC	coordinates of point where correction to potential had maximum absolute value
MAX· CORRECT	maximum value of calculated correction to potential. This correction was introduced at the point (IC, JC).
CIRCULATION	value of circulation Γ
RELAX· COEF	value of relaxation factor RLX used in last iteration sweep (eq. (54)).
ISTG	number of leading-edge stagnation point. From that point the next iteration sweep will start proceeding along the airfoil suction surface to the trailing edge and then again from ISTG along the pressure surface to the trailing edge. In such a way the problems of marching upstream in the locally supersonic flow and the consequent introduction of negative artificial viscosity are avoided.
NSUP	total number of supersonic points in flow field

When the absolute value of the normalized convergence rate

$$(\Gamma^{n+1} - \Gamma^{n})/\Gamma^{n}$$

becomes smaller than CONVER, the iterative process on that particular grid will terminate. For $\Gamma = 0$ (when the flow is nonlifting) the iterative process on each grid will terminate after ITER = ITRMAX on that particular grid. The printout will then be continued by listing the following values on the blade surface:

X	x' coordinate of point on airfoil surface. (The airfoil has been rotated by the stagger angle TWIST.)
Y	y' coordinate of point on airfoil surface

XNORM x' coordinate normalized with actual chord

CP coefficient of pressure

$$C_p = \frac{p - p_{-\infty}}{\frac{1}{2}\rho_{-\infty} q_{-\infty}^2}$$

DENS local density normalized with respect to density at upstream infinity

MACH local value of Mach number

Q/QINF ratio of local speed to speed at upstream infinity

$$Q/QINF = \left[\left(u^2 + v^2\right)/q_{-\infty}^2\right]^{1/2}$$

If PMESH was given as different from PMESH = 1 in the input data, subroutine MESH will refine the basic mesh so that the new mesh will have twice as many mesh cells in the X and Y directions as the previous mesh. The printout will continue with a listing of ITER, IR, JR, . . ., etc., on that new mesh.

Finally, when the last iteration sweep is completed on the last specified mesh, the chart of the Mach numbers (multiplied by 10) in the entire flow field will be printed. The first horizontal line of numbers ranging from j = 2 to J = MAXY corresponds to the elliptic mesh layers enveloping the airfoil. Here J = 2 corresponds to the mesh layer along the periodic boundary; MAXY corresponds to the mesh layer along the surface of the airfoil.

The first column of numbers on this chart designates the number of the mesh point, with I = 2 corresponding to the (lower) trailing-edge point. The Mach number chart will be deleted from the printout if the Mach number at upstream infinity is

$$M_{-\infty} < 0.0011.$$

The Mach number chart is followed by the values of the Mach number, density, and free-stream angle at downstream infinity calculated after the end of the last iteration sweep on the final grid. They are followed by the final results of the calculation, a list of the flow parameters on the airfoil surface and the C_p-distribution chart.

RESULTS

The computer program CAS2D was tested four times. All calculations were performed on three consecutively refined grids measuring 24×6, 48×12, and 96×24 mesh cells, respectively. The relaxation parameter used on the coarse grid was RLX = 1.65. The convergence criterion for the circulation rate was CONVER = $1. *10^{-6}$ on the coarse grid. The maximum allowable numbers of iterations on the three grids were specified as

TITR1 = 120. TITR2 = 60. TITR3 = 30.

The remaining input parameters for each test case are summarized in table I. The last column in that table gives references that provide results widely accepted as being exact. A private communication from D. A. Caughey of Cornell University provides the results for an isolated NACA 0012 airfoil in free air. Figure 8 shows that these results are in excellent agreement with the results obtained by using CAS2D for PITCH = 3.6 (the nonlifting incompressible test, test case 1).

Figure 9 gives the comparison between the second test case, the lifting incompressible test, and the results of reference 9. The agreement is again excellent despite the fact that the airfoil used is cusped. Figure 10 compares the nonlifting transonic, shocked test case, test case 3, with the results obtained by D. A. Caughey. There is practically no difference between the results of the fully conservative and quasi-conservative schemes for shocks of that strength. This is in excellent agreement with the theoretical analysis performed by Caughey (ref. 10).

The fourth test case was done on a shockless cascade of airfoils obtained by J. Sanz of Langley Research Center (ICASE)(private communication), who used a computer code developed by Bauer, Garabedian, and Korn (ref. 8). This airfoil had an open trailing edge extending to downstream infinity. After the trailing edge had been rounded (closed), the proper flow parameters at the downstream infinity were obtained by using AR = 1.023 in the input. The agreement between the results of CAS2D and the results of Sanz are very good (fig. 11). The discrepancy of results near the trailing edge is a consequence of the geometric modifications in that region.

Lewis Research Center,
National Aeronautics and Space Administration,
Cleveland, Ohio, March 5, 1980,
505-32.

APPENDIX - LIMITATIONS OF CAS2D CODE

Each user should be aware of certain limitations in the CAS2D code. A gap-chord ratio less then approximately PITCH = 0.65 often leads to problems associated with the mesh generation routines. Keeping the stagger angle TWIST within the range

$$+45^{\circ} < \text{TWIST} < -45^{\circ}$$

avoids large mesh distortions when PITCH is small. The Mach number at upstream infinity, FMACH, must be less than unity, and airfoil camber should not be excessive. Four example cases of input data are shown in figures 12 to 15.

The format in which the input should be given is as follows:

Card	Format
1	20A4
2 to 7	9X, E12.5, 7X, E12.5, 7X, E12.5
8 to end	2F10.6

REFERENCES

1. Dulikravich, D. S.: Numerical Calculation of Inviscid Transonic Flow Through Rotors and Fans. Ph. D. Thesis, Cornell University, 1979.
2. Steger, J. L.; and Baldwin, B. S.: Shock Waves and Drag in the Numerical Calculation of Isentropic Transonic Flow. NASA TN-6997, 1972.
3. Caughey, D. A.; and Jameson, A.: Numerical Calculation of Transonic Potential Flow About Wing-Fuselage Combinations. AIAA Paper 77-677, June 1977.
4. Jameson, A.: Iterative Solution of Transonic Flows over Airfoils and Wings, Including Flows at Mach 1. Commun. Pure Appl. Math., vol. 27, May 1974, pp. 283-309.
5. Jameson, A.: Transonic Flow Calculations. Computational Fluid Dynamics, Vol. 1 - Numerical Analysis of Transonic and Physiological Flows. VKI-LECTURE-SERIES-87-VOL-1, Von Karman Institute for Fluid Dynamics (Rhode-Saint-Genese, Belgium), 1976, pp. 1.1-5.84.
6. Kober, H.: Dictionary of Conformal Representations. Dover Publications, Inc., 1957, p. 131.
7. Spiegel, Murray R.: Mathematical Handbook of Formulas and Tables. Schaum's Outline Series, McGraw-Hill Book Co., Inc., 1968.
8. Bauer, F.; Garabedian, P.; and Korn, D.: Supercritical Wing Sections 111. Lecture Notes in Economics and Mathematical Systems, Vol. 150, Springer-Verlag (Berlin), 1977.
9. Gostelow, J. P.: Potential Flow Through Cascades - A Comparison Between Exact and Approximate Solutions. ARC-CP-807, Liverpool Univ. (England), 1965.
10. Caughey, D. A.; and Jameson, A.: Recent Progress in Finite-Volume Calculations for Wing-Fuselage Combinations. AIAA Paper 79-1513, July 1979.

TABLE I. - INPUT DATA FOR FOUR TEST CASES

Test case	Airfoil	Mach number of free stream at upstream infinity, FMACH	Angle between free stream and x axis at upstream infinity, ALPHA1, deg	Stagger angle, TWIST, deg	Angle between free stream and x axis at downstream infinity, ALPHA2, deg	Gap-chord ratio, PITCH,	Ratio of blade passage exit area to inlet area, AR	Comparison with reference
1	NACA 0012	0.001	0	0	0	3.6	1.0	(a)
2	Gostelow (cusped)	.001	53.5	-37.5	30.0249	.990157	1.0	9
3	NACA 0012	.8	0	0	0	3.6	1.0	(a)
4	Jose Sanz (shockless)	.711	30.81	-9.32968	-.09	1.02824	1.023	(b)

[a]Private communication from D. A. Caughey of Sibley School of Mechanical and Aerospace Engineering, Cornell University.

[b]Private communication from J. Sanz of ICASE, Langley Research Center.

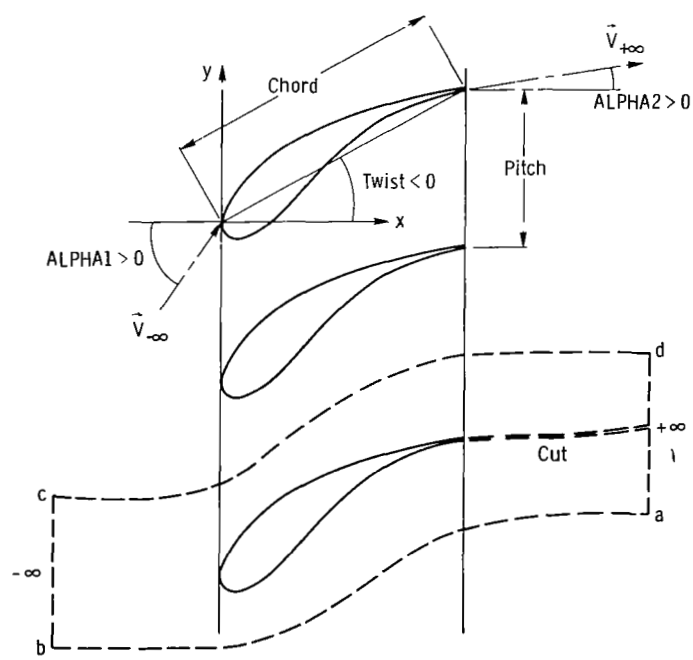

Figure 1. - Planar cascade of airfoils.

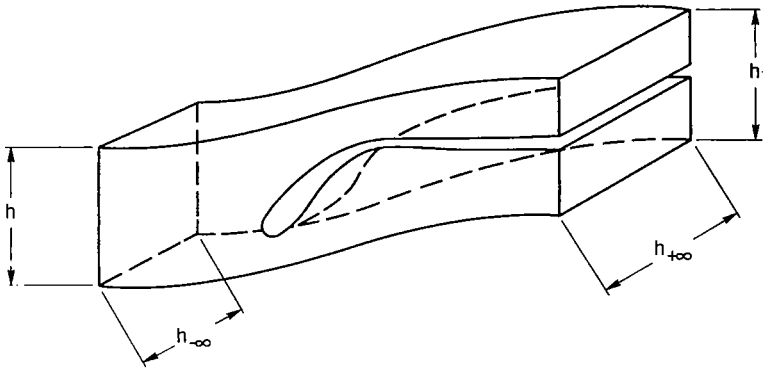

Figure 2. - Quasi-three-dimensional effect.

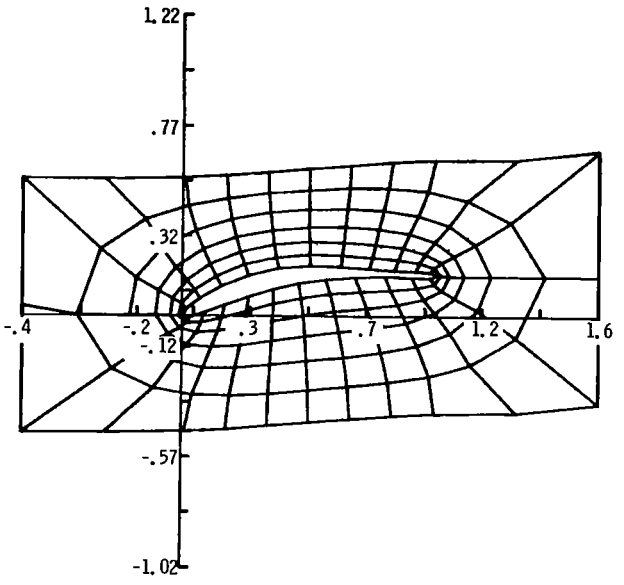

Figure 3. - Computational mesh in physical plane.

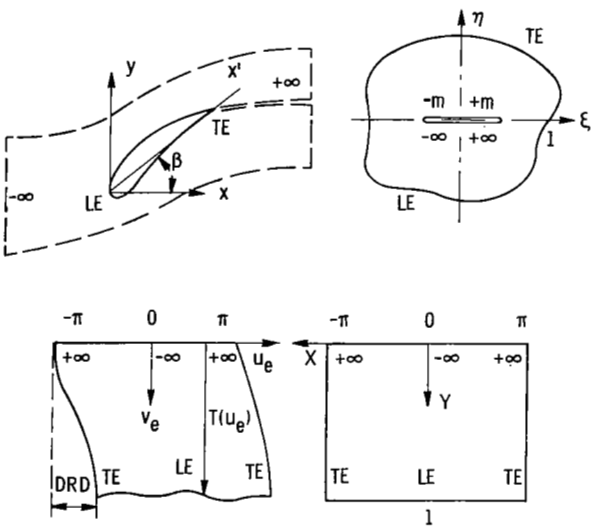

Figure 4. - Geometric transformation sequence, where TE denotes trailing edge and LE denotes leading edge.

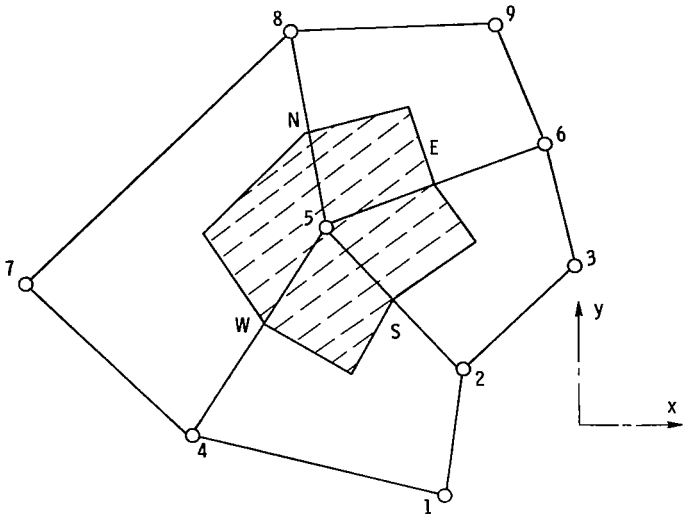

Physical (x, y) space

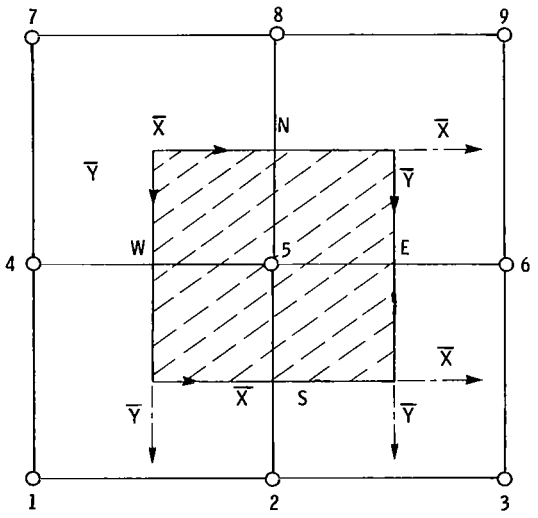

Computational (X, Y) space

Figure 5. - Auxiliary and elementary mesh cells.

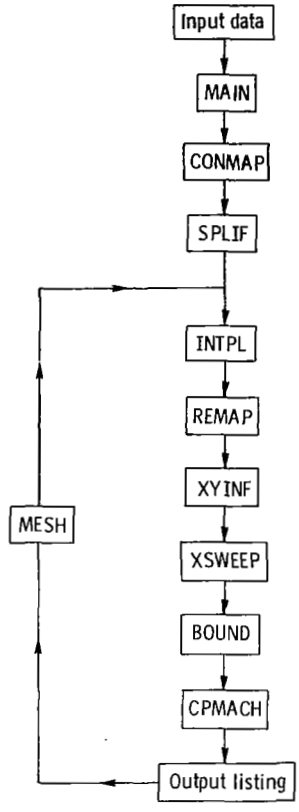

Figure 6. - Block diagram of CAS2D program.

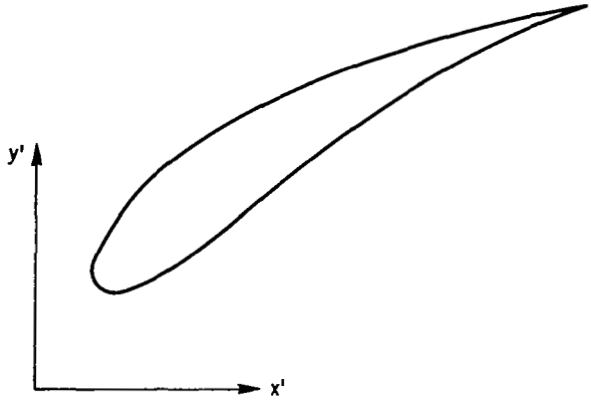

Figure 7. - Input coordinate system.

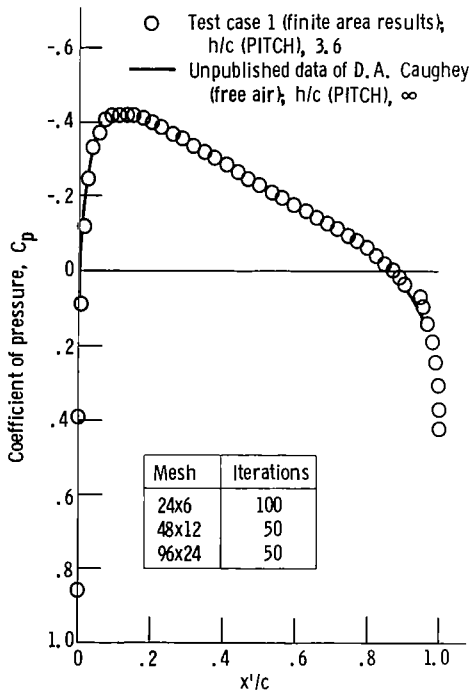

Figure 8. - Comparison of nonlifting incompressible test case (test case 1) with unpublished data of D.A. Caughey of Sibley School of Mechanical and Aerospace Engineering, Cornell University. Airfoil, NACA 0012; Mach number of free stream at upstream infinity, $M_{-\infty}$ (FMACH), 0.001; stagger angle between x axis and airfoil chord line, β(TWIST), 0^0; angle between free stream and x axis at upstream infinity, $\alpha_{-\infty}$ (ALPHA1), 0^0; angle between free stream and x axis at downstream infinity, $\alpha_{+\infty}$ (ALPHA2), 0^0; ratio of inlet area to exit area of blade-to-blade passage, AR, 1.0.

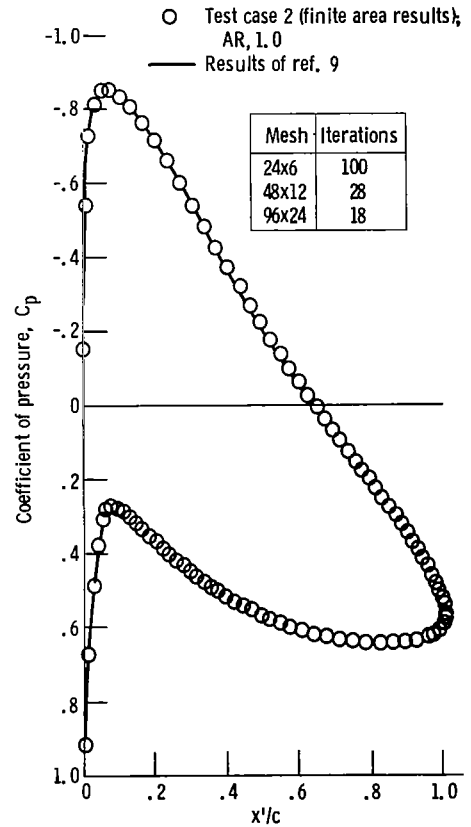

Figure 9. - Comparison of lifting uncompressible test case (test case 2) with results of reference 9. Airfoil, Gostelow cusped; Mach number of free stream at upstream infinity, $M_{-\infty}$ (FMACH), 0.001; stagger angle between x axis and airfoil chord line, β (TWIST), -37.5^0; angle between free stream and x axis at upstream infinity, $\alpha_{-\infty}$ (ALPHA1), 53.5^0; angle between free stream and x axis at downstream infinity, $\alpha_{+\infty}$ (ALPHA2), 30.0249^0; gap-chord ratio, h/c (PITCH), 0.990157.

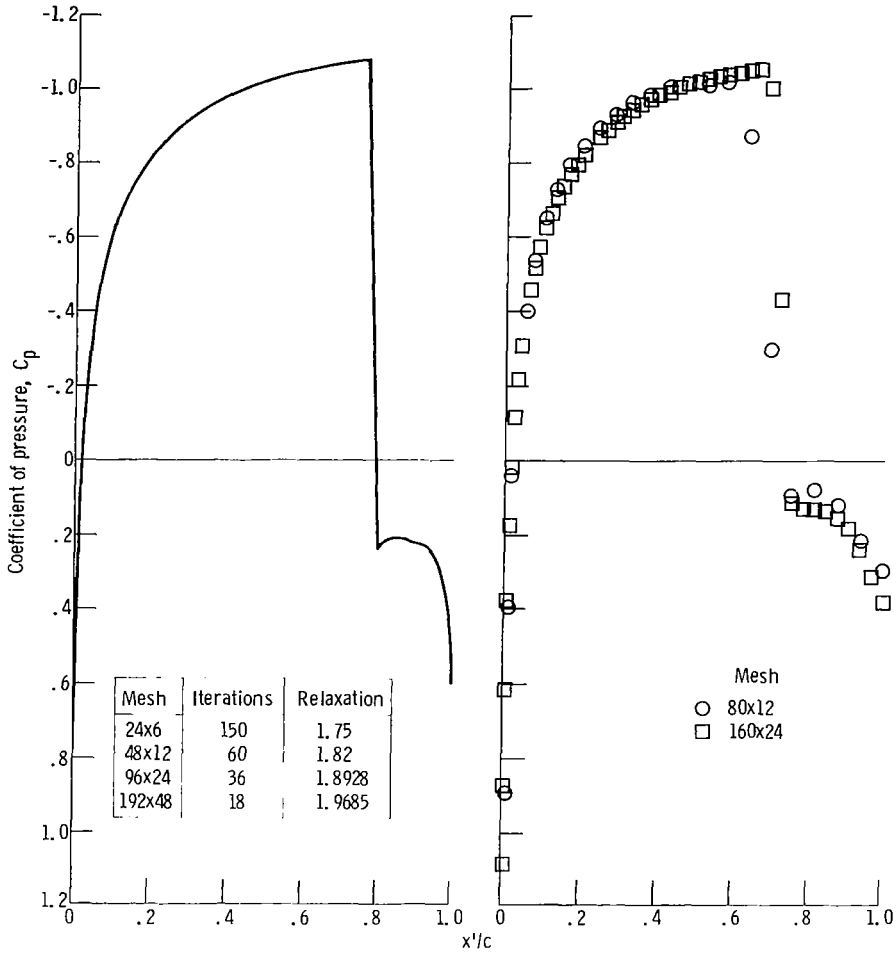

(a) Test case 3 (finite area results).

(b) Unpublished data of D. A. Caughey.

Figure 10. - Comparison of nonlifting transonic-shocked test case (test case 3) with unpublished data of D. A. Caughey of Sibley School of Mechanical and Aerospace Engineering, Cornell University. Airfoil, NACA 0012; Mach number of free stream at upstream infinity, $M_{-\infty}$ (FMACH), 0.8; stagger angle between x axis and airfoil chord line, β (TWIST), 0°; angle between free stream and x axis at upstream infinity, $\alpha_{-\infty}$ (ALPHA1), 0°; angle between x axis and airfoil chord line at downstream infinity, $\alpha_{+\infty}$ (ALPHA2), 0°; gap-chord ratio, h/c (PITCH), 3.6; ratio of inlet area to exit area of blade-to-blade passage, AR, 1.0.

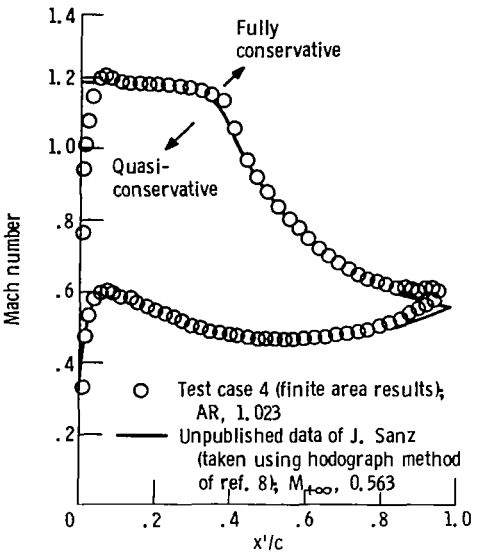

Figure 11. - Comparison of lifting transonic shockless test case (test case 4) with unpublished data of J. Sanz of ICASE, Langley Research Center. Airfoil, J. Sanz shockless; Mach number of free stream at upstream infinity, $M_{-\infty}$ (FMACH), 0.711; stagger angle between x axis and airfoil chord line, β (TWIST), -9.32968^{0}; angle between free stream and x axis at upstream infinity, $\alpha_{-\infty}$ (ALPHA1), 30.81^{0}; angle between x axis and free stream at downstream infinity, $\alpha_{+\infty}$ (ALPHA2), -0.09^{0}; gap-chord ratio, h/c (PITCH), 1.02824.

```
0000100   NACA 0012 - INCOMPRESSIBLE NONLIFTING CASE
0000200   XCELL = 0.20000D+02YCELL = 0.05000D+02PMESH = 4.00000D+00
0000300   ALPHA1= 0.00000D+00TWIST = 0.00000D+00ALPHA2= 0.00000D+00
0000400   PITCH = 3.60000D+00RO1   = 0.01580D+00RO2   = 0.00050D+00
0000500   FMACH = 0.00100D+00RLX   = 1.72000D+00AR    = 1.00000D+00
0000600   TITR1 = 1.50000D+02TITR2 = 0.60000D+02TITR3 = 0.36000D+02
0000700   POINTS= 0.18000D+02GAMMA = 1.40000D+00CONVER= 1.00000D-06
0000800   1.000000  0.000000
0000900   0.950000 -0.009070
0001000   0.900000 -0.014480
0001100   0.800000 -0.026230
0001200   0.700000 -0.036640
0001300   0.600000 -0.045630
0001400   0.500000 -0.052940
0001500   0.400000 -0.058030
0001600   0.300000 -0.060020
0001700   0.250000 -0.059410
0001800   0.200000 -0.057370
0001900   0.150000 -0.053450
0002000   0.100000 -0.046830
0002100   0.075000 -0.042000
0002200   0.050000 -0.035550
0002300   0.025000 -0.026150
0002400   0.012500 -0.018940
0002500   0.000000  0.000000
```

Figure 12. - Input data for incompressible nonlifting test case.

```
0000100   GOSTELOW CUSPED AIRFOIL
0000200   XCELL = 0.24000D+02YCELL = 0.06000D+02PMESH = 4.00000D+00
0000300   ALPHA1= 0.53500D+02TWIST =-0.37500D+02ALPHA2= 3.00249D+01
0000400   PITCH = 9.90157D-01RO1   = 0.01280D+00RO2   = 0.00005D+00
0000500   FMACH = 0.00100D+00RLX   = 1.75000D+00AR    = 1.00000D+00
0000600   TITR1 = 1.50000D+02TITR2 = 0.50000D+02TITR3 = 0.30000D+02
0000700   POINTS= 0.39000D+02GAMMA = 1.40000D+00CONVER= 1.00000D-05
0000800   1.000000  0.000000
0000900   0.998590  0.000390
0001000   0.988070  0.003090
0001100   0.918570  0.017050
0001200   0.816750  0.029510
0001300   0.691660  0.035040
0001400   0.562250  0.031740
0001500   0.425130  0.020330
0001600   0.321980  0.007780
0001700   0.272560  0.001030
0001800   0.232030 -0.004630
0001900   0.165360 -0.013530
0002000   0.110980 -0.019350
0002100   0.057580 -0.021490
0002200   0.030890 -0.019220
0002300   0.015190 -0.015100
0002400   0.005990 -0.009930
0002500   0.000010 -0.000040
0002600   0.001130  0.008660
0002700   0.004610  0.015330
0002800   0.017060  0.028890
0002900   0.035630  0.042360
0003000   0.059530  0.055450
0003100   0.088440  0.067920
0003200   0.122350  0.079540
0003300   0.161610  0.090090
0003400   0.206980  0.099280
0003500   0.259910  0.106710
0003600   0.323170  0.111730
0003700   0.403050  0.113030
0003800   0.521140  0.106280
0003900   0.710520  0.077590
0004000   0.786060  0.060730
0004100   0.826600  0.050520
0004200   0.914960  0.025760
0004300   0.961260  0.011740
0004400   0.987110  0.003830
0004500   0.998680  0.000380
0004600   1.000000  0.000000
```

Figure 13. - Input data for incompressible lifting test case.

```
0000100   NACA 0012 - TRANSONIC NONLIFTING CASE
0000200   XCELL = 0.24000D+02YCELL = 0.06000D+02PMESH = 4.00000D+00
0000300   ALPHA1= 0.00000D+00TWIST = 0.00000D+00ALPHA2= 0.00000D+00
0000400   PITCH = 3.60000D+00RO1   = 0.01580D+00RO2   = 0.00050D+00
0000500   FMACH = 0.80000D+00RLX   = 1.78000D+00AR    = 1.00000D+00
0000600   TITR1 = 1.50000D+02TITR2 = 0.60000D+02TITR3 = 0.36000D+02
0000700   POINTS= 0.18000D+02GAMMA = 1.40000D+00CONVER= 1.00000D-06
0000800   1.000000  0.000000
0000900   0.950000 -0.008070
0001000   0.900000 -0.014480
0001100   0.800000 -0.026230
0001200   0.700000 -0.036640
0001300   0.600000 -0.045630
0001400   0.500000 -0.052940
0001500   0.400000 -0.058030
0001600   0.300000 -0.060020
0001700   0.250000 -0.059410
0001800   0.200000 -0.057370
0001900   0.150000 -0.053450
0002000   0.100000 -0.044830
0002100   0.075000 -0.042000
0002200   0.050000 -0.035550
0002300   0.025000 -0.026150
0002400   0.012500 -0.018940
0002500   0.000000  0.000000
```

Figure 14. - Input data for transonic, shocked nonlifting test case.

```
0000100   JOSE SANZ SHOCKLESS CASCADE - TIP SECTION
0000200   XCELL = 0.24000D+02YCELL = 0.06000D+02PMESH = 3.00000D+00
0000300   ALPHA1= 0.30810D+02TWIST =-9.32968D+00ALPHA2=-0.09000D+00
0000400   PITCH = 1.04400D+00RO1    = 0.01000D+00RO2    = 0.01000D+00
0000500   FMACH = 0.71100D+00RLX    = 1.68000D+00AR     = 1.02600D+00
0000600   TITR1 = 1.20000D+02TITR2 = 0.60000D+02TITR3 = 0.30000D+02
0000700   POINTS= 1.27000D+02GAMMA = 1.40000D+00CONVER= 1.00000D-05
0000800   0.994000  0.171500
0000900   0.990000  0.163000
0001000   0.980000  0.160200
0001100   0.955800  0.161200
0001200   0.908400  0.163200
0001300   0.854600  0.165300
0001400   0.802700  0.166800
0001500   0.754500  0.167100
0001600   0.710900  0.166400
0001700   0.671500  0.164800
0001800   0.635900  0.162600
0001900   0.603500  0.159900
0002000   0.573900  0.156800
0002100   0.546700  0.153400
0002200   0.521700  0.149800
0002300   0.498400  0.146100
0002400   0.476800  0.142200
0002500   0.456600  0.138300
0002600   0.437700  0.134400
0002700   0.419800  0.130400
0002800   0.402900  0.126400
0002900   0.386900  0.122400
0003000   0.372100  0.118100
0003100   0.357800  0.114200
0003200   0.343900  0.110300
0003300   0.330700  0.106400
0003400   0.318000  0.102600
0003500   0.305800  0.098800
0003600   0.294000  0.095000
0003700   0.282600  0.091200
0003800   0.271500  0.087500
0003900   0.260700  0.083800
0004000   0.250200  0.080200
0004100   0.240100  0.076600
0004200   0.230100  0.073000
0004300   0.220400  0.069500
0004400   0.210700  0.066000
0004500   0.201400  0.062600
0004600   0.191900  0.059300
0004700   0.182700  0.055900
0004800   0.173600  0.052500
0004900   0.164700  0.049100
0005000   0.155700  0.045700
0005100   0.146900  0.042400
0005200   0.138000  0.039000
0005300   0.129200  0.035800
0005400   0.120300  0.032400
0005500   0.111600  0.029200
0005600   0.102700  0.025900
0005700   0.094000  0.022700
0005800   0.085100  0.019400
0005900   0.076400  0.016400
0006000   0.067500  0.013300
0006100   0.058900  0.010400
0006200   0.050000  0.007700
0006300   0.041400  0.005200
0006400   0.032500  0.003000
0006500   0.024100  0.001300
0006600   0.015300 -0.000000
0006700   0.007900 -0.000600
0006800   0.000000  0.000000
0006900  -0.007900  0.006900
0007000  -0.006400  0.016500
0007100   0.031100  0.055600
0007200   0.054800  0.072200
0007300   0.082600  0.089600
0007400   0.110300  0.105400
0007500   0.136100  0.119000
0007600   0.158600  0.130000
0007700   0.178400  0.139100
0007800   0.195600  0.146600
0007900   0.210900  0.152900
0008000   0.224500  0.158200
0008100   0.236800  0.162800
0008200   0.247800  0.166800
0008300   0.257900  0.170300
0008400   0.267100  0.173300
0008500   0.275600  0.176000
0008600   0.283400  0.178400
0008700   0.290700  0.180600
0008800   0.297500  0.182500
0008900   0.303900  0.184300
0009000   0.309900  0.185900
0009100   0.315700  0.187400
0009200   0.321100  0.188800
0009300   0.326200  0.190000
0009400   0.331100  0.191200
0009500   0.335700  0.192200
0009600   0.340200  0.193200
0009700   0.344500  0.194100
0009800   0.348600  0.195000
0009900   0.352600  0.195800
0010000   0.356600  0.196500
0010100   0.360500  0.197300
0010200   0.364400  0.198000
0010300   0.368300  0.198600
0010400   0.372200  0.199300
0010500   0.376200  0.199900
0010600   0.380300  0.200500
0010700   0.398700  0.202700
0010800   0.408000  0.204000
0010900   0.417500  0.204900
0011000   0.427700  0.205800
0011100   0.438200  0.206700
0011200   0.449500  0.207400
0011300   0.461200  0.208000
0011400   0.473700  0.208500
0011500   0.486800  0.208800
0011600   0.500800  0.209100
0011700   0.515600  0.209200
0011800   0.531500  0.209100
0011900   0.548600  0.208800
0012000   0.567100  0.208200
0012100   0.587200  0.207400
0012200   0.609400  0.206400
0012300   0.633900  0.205000
0012400   0.661500  0.203200
0012500   0.692500  0.201000
0012600   0.727900  0.198500
0012700   0.768400  0.195500
0012800   0.815100  0.192300
0012900   0.867600  0.189000
0013000   0.922500  0.186200
0013100   0.967700  0.184500
0013200   0.983000  0.184000
0013300   0.990000  0.180500
0013400   0.994000  0.171500
```

Figure 15. - Input data for transonic, shockless lifting test case.

1. Report No.	2. Government Accession No.	3. Recipient's Catalog No.
NASA TP -1705		

4. Title and Subtitle	5. Report Date
CAS2D - FORTRAN PROGRAM FOR NONROTATING BLADE-TO-BLADE, STEADY, POTENTIAL TRANSONIC CASCADE FLOWS	July 1980
	6. Performing Organization Code
7. Author(s)	8. Performing Organization Report No.
Djordje S. Dulikravich	E-253
9. Performing Organization Name and Address	10. Work Unit No.
National Aeronautics and Space Administration Lewis Research Center Cleveland, Ohio 44135	505-32
	11. Contract or Grant No.
12. Sponsoring Agency Name and Address	13. Type of Report and Period Covered
National Aeronautics and Space Administration Washington, D.C. 20546	Technical Paper
	14. Sponsoring Agency Code

15. Supplementary Notes

Djordje S. Dulikravich: NRC-NASA Resident Research Associate.

16. Abstract

An exact, full-potential-equation (FPE) model for the steady, irrotational, homentropic and homoenergetic flow of a compressible, homocompositional, inviscid fluid through two-dimensional planar cascades of airfoils was derived, together with its appropriate boundary conditions. A computer program, CAS2D, was developed that numerically solves an artificially time-dependent form of the actual FPE. The governing equation was discretized by using type-dependent, rotated finite differencing and the finite area technique. The flow field was discretized by providing a boundary-fitted, nonuniform computational mesh. The mesh was generated by using a sequence of conformal mapping, nonorthogonal coordinate stretching, and local, isoparametric, bilinear mapping functions. The discretized form of the FPE was solved iteratively by using successive line overrelaxation. The possible isentropic shocks were correctly captured by adding explicitly an artificial viscosity in a conservative form. In addition, a three-level consecutive, mesh refinement feature makes CAS2D a reliable and fast algorithm for the analysis of transonic, two-dimensional cascade flows.

17. Key Words (Suggested by Author(s))	18. Distribution Statement
Numerical methods Cascade flows Transonic flows Turbomachinery	Unclassified – Unlimited Subject Category 02

19. Security Classif. (of this report)	20. Security Classif. (of this page)	21. No. of Pages	22. Price*
Unclassified	Unclassified	35	A03

* For sale by the National Technical Information Service, Springfield, Virginia 22161

NASA-Langley, 1980